Molecules **2015**, *20*, 9961-9976; doi:10.3390/molecules20069961

OPEN ACCESS

molecules

ISSN 1420-3049

www.mdpi.com/journal/molecules

Article

Interplay between Beryllium Bonds and Anion-π Interactions in BeR_2:C_6X_6:Y^- Complexes (R = H, F and Cl, X = H and F, and Y = Cl and Br)

Marta Marín-Luna [1], Ibon Alkorta [1,*], José Elguero [1], Otilia Mó [2] and Manuel Yáñez [2,*]

[1] Instituto de Química Médica (CSIC), Juan de la Cierva, 3, 28006-Madrid, Spain

[2] Departamento de Química, Módulo 13, Universidad Autónoma de Madrid, Campus de Excelencia UAM-CSIC, Cantoblanco, E-28049 Madrid, Spain

* Authors to whom correspondence should be addressed; E-Mails: ibon@iqm.csic.es (I.A.); manuel.yanez@uam.es (M.Y.); Tel.: +34-562-2900 (I.A.); +34-497-4953 (M.Y.).

Academic Editor: Antonio Frontera

Received: 22 April 2015 / Accepted: 26 May 2015 / Published: 29 May 2015

Abstract: A theoretical study of the beryllium bonds in BeR_2:C_6X_6 (R = H, F, Cl and X = H and F) has been carried out by means of MP2/aug′-cc-pVDZ computational methods. In addition, the ternary complexes BeR_2:C_6X_6:Y^- (Y = Cl and Br) have been analyzed. Geometric, energetic and electronic aspects of the complexes have been taken into account. All the parameters analyzed provide a clear indication of favorable cooperativity in both interactions observed, beryllium bond and aromatic ring:anion interaction.

Keywords: beryllium-π interactions; anion-π interactions; *ab initio* calculations; cooperativity

1. Introduction

In 2002, three independent groups showed theoretically for the first time the possibility of finding attractive anion-π interactions when the π system is electron deficient [1–3], hexafluorobenzene being a paradigmatic case. These theoretical calculations were supported by crystallographic data found in the Cambridge Structural Database (CSD) [1,4]. It was suggested that this novel mode of bonding could be used for developing new receptors for the recognition of anions [2]. Relationships have been found between the aromaticity of perfluoroaromatic compounds and their relative interaction energy with anions [3]. Since then, the number of papers reporting anion-π interactions has become very

large; the reader can consult some reviews or very general papers [5–7] and two books [8,9]. Particularly informative is an experimental paper by Wang and Wang [10] based on 1,3,5-triazine, another of the classical π-deficient systems [2]. Other experimental papers reported solution studies [11] and crystallographic structures [12], both based on the C_6F_5 substituent.

Somewhat related to the anion-π interactions topic is the use of aromatic compounds as charge insulators. Many examples have been reported: Na^+:C_6H_6:F^- and Na^+:C_6F_6:F^- [13]; Li^+:C_6H_6: F^-; K^+:C_6F_6:Br^- [14]; M^+:$C_6H_3F_3$:$C_6H_3F_3$:X^- [15]; M^+:C_6F_6:Cr:C_6H_6:X^- [16]; M^+:C_6H_6:C_6F_6:X^- [17]; cyclopropenyl$^+$:C_6H_6:phenalenyl$^-$ [18]; Na^+:1,3,5-triethynylbenzene: Cl^- [19]; Li^+:C_6R_6:F^-, R = H, F, Cl, Br, OMe [20], and $-Na^+$:$C_6H_3F_3$:Cl^- [21]. These have been extended to other insulators like hexafluoroethane [Na^+:C_2F_6:Cl^-] [22], saturated cycloalkanes like Li^+:adamantane:F^- [23], cationic complexes like ZY_4^+:C_6R_6:YX, example: NH_4^+:C_6H_6:HF [24] as well as anionic complexes as XH:C_2F_4:Y^- [25].

Among the new non-covalent interactions discovered in the last years, beryllium bonds provide very strong complexes [26] and significantly alter the properties of the bonded systems [27–34]. Recently it has been shown that beryllium derivatives can interact with π-systems, such as ethylene or acetylene, to yield rather stable complexes [35]. In the present paper we will explore the structure and stability of the complexes of BeR_2 derivatives with benzene, as the aromatic reference system, and with its hexafluoro derivative, C_6F_6, which should behave as a much weaker Lewis base than the parent C_6H_6. The second part of the paper will be devoted to analyze the similarities and dissimilarities between the complexes formed between these two aromatic compounds and halogen anions, namely Cl^- and Br^-. In the third part we will analyze the effect of the simultaneous interaction of beryllium derivatives and halogen anions with benzene and hexafluorobenzene. A comparison between the binary complexes studied in the first two parts of the paper and the triads contemplated in the third part will allow us to detect possible cooperative effects between both kinds of non-covalent interactions within the triads.

2. Computational Methods

The geometry of the systems has been fully optimized with the MP2 computational method [36] and the aug′-cc-pVDZ basis set. This basis set corresponds to the aug-cc-pVDZ [37] one for the heavy atoms and to the cc-pVDZ one for the hydrogens. Frequency calculations have been carried out at the same computational level to confirm that the structures obtained correspond to energetic minima. All these calculations have been carried out with the Gaussian-09 program [38].

The many-body interaction-energy formalism (MBIE) [39,40] has been applied to obtain one-, two- and three-body contributions to the binding energy. For a ternary complex, the binding energy ΔE can be decomposed into one- (Equation (2)), two- (Equation (3)), and three-body interactions (Equation (4)), as:

$$\Delta E = E(ABC) - \sum_{i=A}^{C} E_m(i) = \sum_{i=A}^{C} \left[E(i) - E_m(i)\right] + \sum_{i=A}^{B} \sum_{j>i}^{C} \Delta^2 E(ij) + \Delta^3 E(ABC) \quad (1)$$

$$E_R(i) = E(i) - E_m(i) \quad (2)$$

$$\Delta^2 E(ij) = E(ij) - \left[E(i) - E(j)\right] \quad (3)$$

$$\Delta^3 E(ABC) = E(ABC) - [E(A) + E(B) + E(C)] - [\Delta^2 E(AB) + \Delta^2 E(AC) + \Delta^2 E(BC)] \quad (4)$$

$E_m(i)$ is the energy of an isolated, optimized monomer, while $E(i)$ is the monomer energy at its geometry in the complex. $E_R(i)$ is the monomer distortion energy. $\Delta^2 E(ij)$ and $\Delta^3 E(ABC)$ are the two- and three-body interaction energies computed at the corresponding geometries in the complex.

The topological analysis of the electron density of the systems has been carried out within the framework of the Atoms in Molecules (AIM) [41,42] methodology with the AIMAll [43] program using the MP2/aug′-cc-pVDZ wavefunction. The electronic properties and charge transfer of the complexes have been analyzed with the NBO method [44] using the NBO 3.1 program [45] at the B3LYP/aug′-cc-pVDZ//MP2/aug′-cc-pVDZ computational level.

The effect of the complexation on the aromaticity of benzene and hexaflurobenzene has been calculated by means of the HOMA index (Equation (5)) [46]. The value of the C-C bond length (1.408 Å) obtained for the isolated benzene at MP2/aug′-cc-pVDZ level has been used as R_{opt} and for the value of α for C-C bonds the reported value has been used [47].

$$HOMA = 1 - \frac{1}{n}\sum_{j=1}^{n} \alpha \left(R_{opt} - R_j \right)^2 \quad (5)$$

3. Results and Discussion

This section has been divided in four parts. In the first part, a brief mention to the electronic properties of the isolated benzene and hexafluorobenzene will be considered. In the second and third parts, the $BeR_2{:}C_6X_6$ and $C_6X_6{:}Y^-$ binary complexes will be respectively discussed. Finally, the last part will be devoted to the ternary $BeR_2{:}C_6X_6{:}Y^-$ complexes. The geometry, energy and molecular graphs of all the systems studied in the present article can be found in Tables S1 and S2 of the Supplementary Materials.

3.1. C_6X_6 Isolated Monomers

The electrostatic properties of the benzene and hexafluorobenzene molecules have been already discussed several times in the literature, especially in the context of their different tendency to form π-complexes [48]. Thus, benzene shows negative values of the electrostatic potential above and below the aromatic ring and tends to form complexes with positively charged groups or hydrogen bond donors [49–53]. In contrast, the electrostatic potential of the C_6F_6 molecule in both sides of the molecular plane presents positive values and consequently tends to form complexes with electron rich groups or anions [48,54]. The differences in the electrostatic potential of these two molecules have been rationalized based on their quadrupole moment [13,55] (Figure 1).

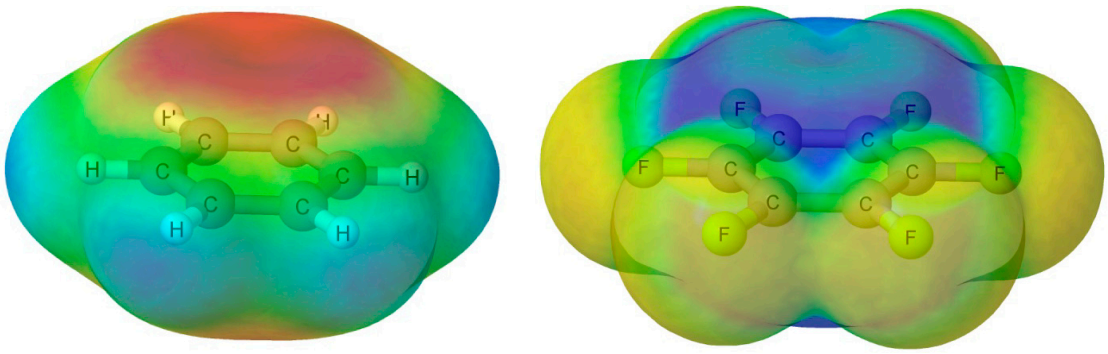

Figure 1. Electrostatic potential on the 0.001 au electron density of the isolated C_6H_6 (**left**) and C_6F_6 (**right**). The most intense red and blue color regions correspond to the −0.02 and +0.03 au values, respectively.

3.2. BeR_2:C_6X_6 Binary Complexes

The binding energy and intermolecular distances of BeR_2:C_6X_6 complexes are listed in Table 1. The binding energies of the complexes with benzene range between −26 kJ/mol and −47 kJ/mol; the $BeCl_2$ and BeH_2 complexes are the most stable and the least stable, respectively. The binding energies for the C_6F_6 range between −13 kJ/mol and −25 kJ/mol and are about half of the analogous ones with C_6H_6.

Table 1. Binding energies (kJ/mol), intermolecular distances (Å) and R-Be-R bond angle (°) of the BeR_2:C_6X_6 binary complexes.

System	Eb	Be···Z*	> R-Be-R	System	Eb	Be···Z*	> R-Be-R
BeH_2:C_6H_6	−25.7	2.575	157.5	BeH_2:C_6F_6	−13.1	2.945	179.0
BeF_2:C_6H_6	−41.4	2.214	146.4	BeF_2:C_6F_6	−15.8	2.916	178.6
$BeCl_2$:C_6H_6	−46.7	2.182	139.7	$BeCl_2$:C_6F_6	−24.6	3.213	177.7

Z* represents the middle of the closest C-C bond of the aromatic system.

The molecular graph of the $BeCl_2$:C_6H_6 and $BeCl_2$:C_6F_6 complexes have been represented in Figure 2, as a suitable case for BeR_2:C_6H_6 and BeR_2:C_6F_6 systems. Clear differences are observed between the two families of complexes. In complexes with C_6H_6, the beryllium atom of the BeR_2 derivatives is located above and close to one of the C-C bonds and slightly out of the aromatic ring while in the C_6F_6 family the Be is far from the C-C bond and placed close to the center of the aromatic ring.

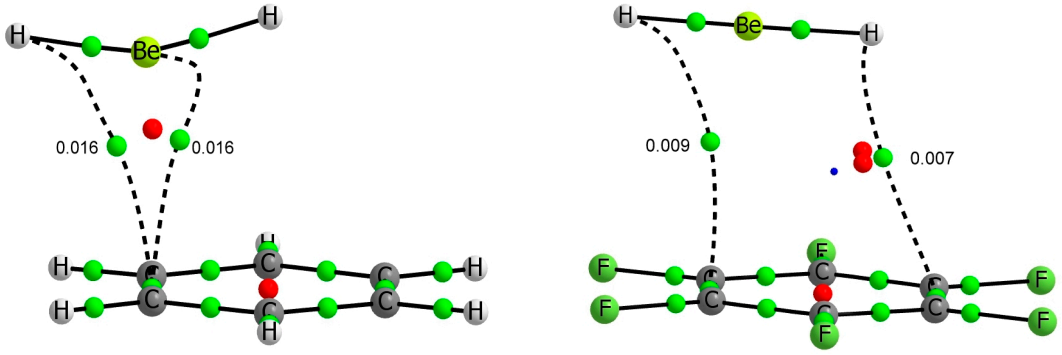

Figure 2. *Cont.*

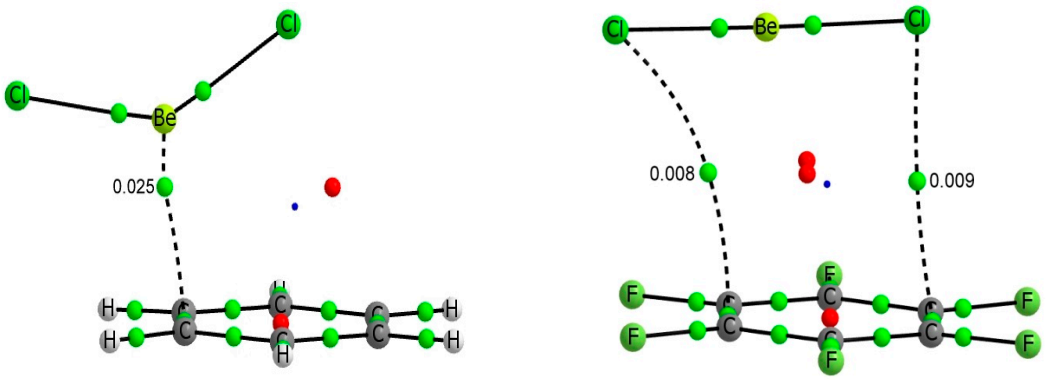

Figure 2. Molecular graph of $BeR_2:C_6H_6$ (R = H, Cl) (**left**) and $BeR_2:C_6F_6$ (R = H, Cl) (**right**) binary complexes. Green, red and blue dots denote BCPs, ring critical points and cage critical points respectively. The value of the electron density at the intermolecular BCP is indicated.

The NBO analysis offers some clue on the origin of the aforementioned differences between $BeR_2:C_6H_6$ and $BeR_2:C_6F_6$ complexes. In both cases the aromatic moiety behaves as a Lewis base with respect to the BeR_2 moiety, since a clear charge donation from the occupied π_{cc} orbitals of the aromatic into the empty p orbitals of Be and into the σ_{BeR}* antibonding orbital is detected from the calculated second order orbital perturbation energies. The former are responsible for the bending undergone by the BeR_2 moiety and the latter for the lengthening of the Be-R distances when BeR_2 forms part of the complex. The NBO analysis shows that for C_6H_6 complexes, the larger contribution comes from a couple of C=C bonds, reflecting that the orbital interaction energies strongly depend on the overlap of the interacting occupied and empty orbitals. Clearly, the specific interaction with two of the CC bonds is privileged with respect to an equal interaction with the six bonds because in the first situation the overlap is much more efficient. In the case of the C_6F_6, the aforementioned interactions are much weaker, since C_6F_6 is a much poorer electron donor than C_6H_6. Indeed, as indicated in Table 2, the natural charges obtained within the NBO approach clearly show that the charge transfer from the aromatic systems towards the beryllium derivatives, is about three times larger when the aromatic is benzene than when it is C_6F_6.

Table 2. NBO charges (e) of the aromatic system within the $BeR_2:C_6X_6$ complexes.

	NBO Charges (e)		**NBO Charges (e)**
$BeH_2:C_6H_6$	0.048	$BeH_2:C_6F_6$	0.017
$BeF_2:C_6H_6$	0.066	$BeF_2:C_6F_6$	0.005
$BeCl_2:C_6H_6$	0.116	$BeCl_2:C_6F_6$	0.012

However, also in C_6F_6 complexes there is a tendency to privilege the donation for only one couple of CC bonds. Actually, as shown in Figure 2, the BeR_2 moiety does not sit strictly above the center of the ring, but it is also slightly displaced towards one of its CC bonds. However, since the interactions for C_6F_6 are much weaker than for benzene, the distance between both moieties is much longer, and the overlap does not privilege significantly the interaction with a specific pair of CC bonds, with respect to the others, leading to a more centered position of the BeR_2 subunit. The fact that C_6F_6 is a

much poorer electron donor than C_6H_6 is also clearly mirrored on the fact that in the C_6H_6 complex, the disposition of the three atoms of the BeR_2 molecule is far from linearity, reaching R-Be-R angles of 140° in the strongest complex, while in the complexes with C_6F_6 the change of this angle is very small (less than 2.5°).

It is worth noting that the BeR_2:C_6F_6 complexes with the beryllium atom along the C_6 symmetry axes, which have a C_{2v} symmetry, present one imaginary frequency and a very small relative energy (less than 2.0 kJ/mol) with respect to the equilibrium conformation, corresponding to a transition state between two identical structures.

In line with the NBO analysis discussed above, the AIM approach shows the existence of just one intermolecular BCP between the beryllium atom and the centre of a C-C bond for complexes involving benzene (Figure 2). The values of the electron density at these BCPs range between 0.016 (BeH_2) and 0.025 au ($BeCl_2$). Positive values of the Laplacian and negative total energy density (between −0.003 and −0.006 au) are found in the BCPs (see Table 3), confirming that these interactions have a certain covalent character [56].

In the BeR_2:C_6F_6 complexes, mentioned above, the interaction is much weaker and more delocalized, the intermolecular BCPs link the R atoms with the aromatic ring through two opposite C-C bonds. The electron density at the BCPs is rather small (between 0.009 and 0.007 au) and the Laplacian and total energy density are positive or nearly zero (Table 3).

Table 3 AIM parameters (in au) for the BCPs corresponding to the intermolecular interactions in the BeR_2:C_6X_6 binary systems, the electron density, ρ_{BCP}, its Laplacian, $\nabla^2\rho_{BCP}$, and the total electron energy density, H_{BCP}.

System	ρ_{BCP}	$\nabla^2\rho_{BCP}$	H_{BCP}	Interaction
BeH_2:C_6H_6	0.0157	0.0184	−0.0028	Be···π
BeF_2:C_6H_6	0.0218	0.0409	−0.0052	Be···π
$BeCl_2$:C_6H_6	0.0247	0.0577	−0.0059	Be···π
BeH_2:C_6F_6	0.0085	0.0153	−0.0001	H··· π
	0.0067	0.0192	0.0008	H··· π
BeF_2:C_6F_6	0.0091	0.0263	0.0008	F··· π
	0.0084	0.0320	0.0012	F··· π
$BeCl_2$:C_6F_6	0.0079	0.0180	0.0004	Cl··· π
	0.0085	0.0240	0.0008	Cl··· π

The calculated HOMA aromaticity indexes for these complexes (See Table S3 of the Supplementary Materials) are very similar to the corresponding isolated aromatic molecules, being the largest differences 0.01 units.

The application of the MBIE partition method shows that for both families of compounds the distortion energy of the aromatic ring is very small, as it is also for the BeR_2 systems in the complexes with C_6F_6 (See Table 4). In contrast, the distortion energies of the BeR_2 molecules in the complexes with C_6H_6 present values between 11 and 39 kJ/mol in agreement with the geometrical perturbation already discussed. Consequently, the interaction energy (Δ^2E) of these complexes reaches values up to −87 kJ/mol in the C_6H_6:$BeCl_2$ case while in the ones with C_6F_6 the values of Δ^2E are about four times smaller and very similar to those of the binding energies.

Table 4. Many body Interaction energy (MBIE) partition terms (kJ/mol) in the $BeR_2:C_6X_6$ binary systems.

System	Er(Ar)	Er(BeR_2)	$\Delta^2E(BeR_2:C_6H_6)$	System	Er(Ar)	Er(BeR_2)	$\Delta^2E(BeR_2:C_6F_6)$
$BeH_2:C_6H_6$	0.2	10.7	−36.6	$BeH_2:C_6F_6$	0.16	0.03	−13.3
$BeF_2:C_6H_6$	0.5	26.3	−68.2	$BeF_2:C_6F_6$	0.3	0.1	−16.2
$BeCl_2:C_6H_6$	0.9	39.0	−86.6	$BeCl_2:C_6F_6$	0.3	0.05	−24.9

3.3. $C_6X_6:Y^-$ Binary Complexes

As expected from the characteristics of the molecular electrostatic potential discussed above, the equilibrium structure for $C_6H_6:Y^-$ complexes is totally different from that of C_6F_6, in agreement with previous reports [3,57–59]. In the C_6H_6 complexes, the anion is located in the molecular plane, interacting simultaneously with two hydrogen atoms, whereas in the $C_6F_6:Y^-$ complexes the anion sits on the C_6 symmetry axis and above the plane of the molecule. Figure 3 shows the molecular graph of two representative $C_6X_6:Y^-$ complexes.

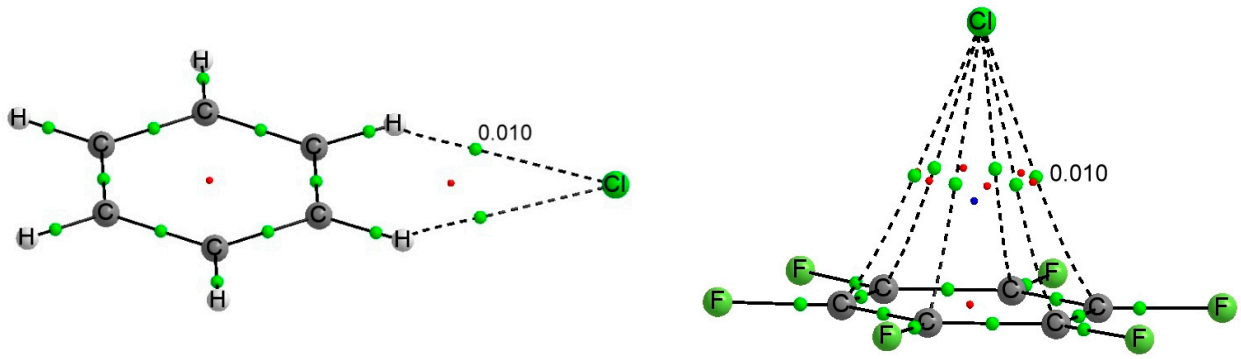

Figure 3. Molecular graph of the $C_6H_6:Cl^-$ (**left**) and $C_6F_6:Cl^-$ (**right**) complexes. Green, red and blue dots denote BCPs, ring and cage critical points respectively. The value of the electron density at the intermolecular BCP is indicated.

The binding energies of these complexes (Table 5) show that the $C_6F_6:Y^-$ complexes are almost twice more stable than the $C_6H_6:Y^-$ ones, in contrast with the results obtained for the $BeR_2:C_6X_6$ complexes, simply because in the complexes with BeR_2 the aromatic ring behaves as a Lewis base *versus* a rather strong Lewis acid, whereas in the complexes with Y^- they behave as a Lewis acid, which can only accept electrons in the π^* antibonding orbitals. The nature of the halide has a small effect on the binding energy, the complexes with chloride being slightly more stable than with bromide. The MBIE partition (Table 4) shows very small distortion energies for the aromatic systems and consequently, the interaction energies (Δ^2E) are very similar to the binding ones.

The molecular graph of these complexes (see Figure 3 for two examples) shows two degenerate Y···H BCPs in the $C_6H_6:Y^-$ complexes, corresponding to the two hydrogen bonds between the halogen anion and the CH groups of benzene, and six Y···C BCP in $C_6F_6:Y^-$. Those BCPs show similar values of the electron density, 0.010 au for the chloride complexes and 0.009 au for the bromide ones. In all cases, the BCPs show positive values of the Laplacian and total energy density.

Table 5. Binding energy (kJ/mol), intermolecular distance (Å), distortion energy and Δ^2E (kJ/mol) in the $C_6X_6:Y^-$ binary systems within the MBIE partition method.

System	Eb	Y···HC	Er(C_6H_6)	$\Delta^2E(C_6H_6:Y)$	System	Eb	Y···Z*	Er(C_6F_6)	$\Delta^2E(C_6F_6:Y)$
$C_6H_6:Br^-$	−34.4	2.902	1.2	−35.6	$C_6F_6:Br^-$	−65.8	3.433	0.7	−66.6
$C_6H_6:Cl^-$	−35.9	2.743	1.6	−37.5	$C_6F_6:Cl^-$	−67.1	3.290	0.9	−67.9

Z* represents the middle of one of the C-C bonds of the aromatic system.

The NBO analysis indicates a larger charge transfer for the $C_6H_6:Y^-$ complexes (−0.026 and −0.027 e, for Y = Br and Cl, respectively) than for the $C_6F_6:Y^-$ ones (−0.013 and −0.012 e), as a consequence of the rather different nature of both kinds of interactions, since, as indicated above the former are stabilized through intermolecular C-H···Y^- hydrogen bonds and the latter through Y^--π interactions. Coherently, the second order perturbation analysis indicates a charge transfer in the $C_6H_6:Y^-$ complexes from the lone pairs of the anions towards the σ_{CH}* antibonding orbitals with interaction energies up to 7.4 kJ/mol, while in the $C_6F_6:Y^-$ ones, the expected charge transfer between the lone pair of the anions and the π_{CC}* antibonding orbitals of the aromatic systems is very small (<0.7 kJ/mol).

3.4. $BeR_2:C_6X_6:Y^-$ Ternary Complexes

The binding energy and intermolecular distances of the $BeR_2:C_6X_6:Y^-$ (R = H, F, Cl; X = H, F; Y = Cl, Br) ternary complexes have been listed in Table 6. The molecular graphs of two representative ternary complexes have been represented in Figure 4.

Table 6. Binding energy (kJ/mol), intermolecular distances (Å) and R-Be-R bond angle (°) of the ternary complexes. The variations with respect to the corresponding binary complexes are also added.

System	Eb	Be···Z*	ΔBe···Z*	Y···Z*	ΔY···Z*	∠ R-Be-R	Δ∠ R-Be-R
$BeH_2:C_6H_6:Br^-$	−80.3	2.185	−0.390	2.820	−0.082	145.7	−11.8
$BeH_2:C_6H_6:Cl^-$	−83.2	2.177	−0.398	2.658	−0.085	145.2	−12.3
$BeF_2:C_6H_6:Br^-$	−104.6	2.089	−0.125	2.802	−0.100	138.1	−8.3
$BeF_2:C_6H_6:Cl^-$	−107.9	2.084	−0.130	2.639	−0.104	137.7	−8.7
$BeCl_2:C_6H_6:Br^-$	−118.7	2.042	−0.140	2.778	−0.124	132.0	−7.7
$BeCl_2:C_6H_6:Cl^-$	−122.4	2.034	−0.148	2.616	−0.127	131.7	−8.0
$BeH_2:C_6F_6:Br^-$	−96.7	2.413	−0.532	3.204	−0.229	155.8	−23.2
$BeH_2:C_6F_6:Cl^-$	−99.0	2.396	−0.549	3.031	−0.259	154.8	−24.2
$BeF_2:C_6F_6:Br^-$	−112.8	2.270	−0.646	3.156	−0.277	144.6	−34.0
$BeF_2:C_6F_6:Cl^-$	−115.6	2.261	−0.655	2.990	−0.300	143.9	−34.7
$BeCl_2:C_6F_6:Br^-$	−122.5	2.253	−0.960	3.126	−0.307	137.9	−39.8
$BeCl_2:C_6F_6:Cl^-$	−125.8	2.242	−0.971	2.957	−0.333	137.2	−40.5

Z* represents the middle of the closest C-C bond of the aromatic system.

The binding energies in the ternary complexes range between −80 and −126 kJ/mol. The C_6F_6 complexes are always more stable than the analogous with C_6H_6. As in the case of the binary complexes, the ranking based on the beryllium derivative is $BeH_2 > BeF_2 > BeCl_2$ and the difference between the binding energy in the chloride and bromide complexes is small, the chloride complexes

always being more stable than the bromide ones. An excellent linear correlation is obtained between the binding energies in the C_6F_6 *vs.* the C_6H_6 series ($R^2 = 0.999$).

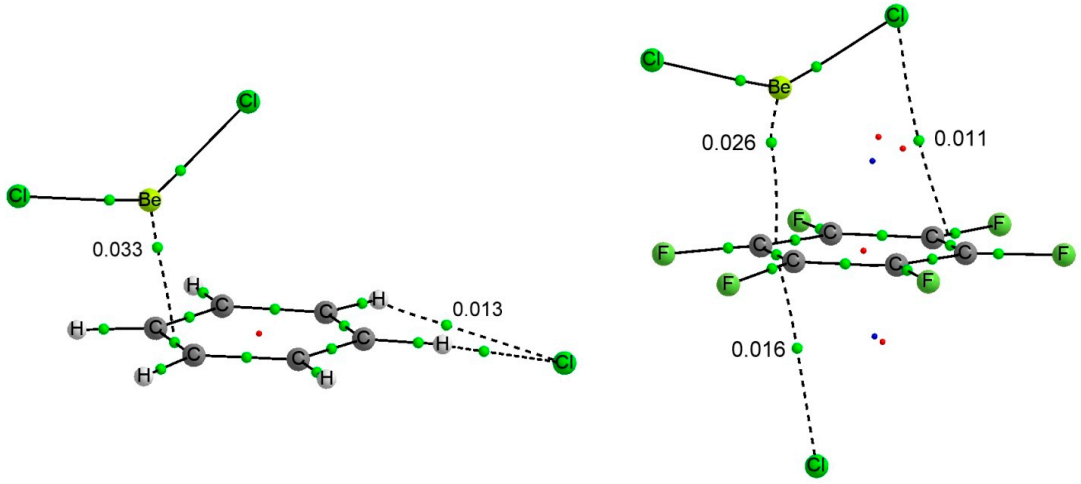

Figure 4. Molecular graph of $BeCl_2$:C_6H_6:Cl^- (**left**) and $BeCl_2$:C_6F_6:Cl^- (**right**). The value of the electron density at the intermolecular BCPs is indicated.

The geometrical parameters listed in Table 6 already provide some clues about the cooperativity in the ternary complexes. The intermolecular distances between the aromatic systems and the beryllium derivatives are reduced up to 0.40 Å in the C_6H_6 series and up to 0.97 Å in the C_6F_6 ones when comparing to the corresponding binary complexes. In C_6H_6 complexes, the larger effects are observed for complexes with BeH_2 and for the $BeCl_2$ for C_6F_6 complexes. Similar shortening is observed for the intermolecular distances between the anions and the aromatic rings. The larger effect observed in both series corresponds to the complexes with $BeCl_2$ being the calculated shortening 0.13 and 0.30 Å in the C_6H_6 and C_6F_6 series, respectively.

Another geometrical parameter that changes from the binary to the ternary complexes is the R-Be-R bond angle which is always smaller in the latter ones. The largest effect is observed in the $BeCl_2$:C_6F_6:Y^- complexes, where the variation of the R-Be-R bond angle on going from the binary to the ternary complexes is 40°.

As in the case of the binary complexes, the calculated HOMA aromaticity indexes for the ternary complexes (See Table S3) are almost identical to those of the corresponding isolated aromatic molecules, being the largest differences 0.02 units.

The MBIE partition terms of the ternary complexes have been gathered in Table 7. The distortion energy in the aromatic molecules is small in all cases (between +1.7 and +4.3 kJ/mol), but larger than in binary complexes, while those of the beryllium derivatives complexed with C_6H_6 range between +26 and +59 kJ/mol and in the complexes with C_6F_6 between +12 and +44 kJ/mol, are also larger than in the binary complexes. The three Δ^2E terms and the Δ^3E one for all the compounds are negative. The largest stabilization energy is the $\Delta^2E(BeR_2{:}Ar)$ for the C_6H_6 complexes and $\Delta^2E(Ar{:}Y)$ for the C_6F_6 ones. For the C_6H_6 complexes the second most important term is the $\Delta^2E(Ar{:}Y)$ followed by the $\Delta^3E(BeR_2{:}Ar{:}Y)$ one, the least important one being the $\Delta^2E(BeR_2{:}Y)$. In the C_6F_6 complexes, $\Delta^2E(BeR_2{:}Y)$ is of similar magnitude to that of $\Delta^2E(BeR_2{:}Ar)$ in the BeR_2:C_6F_6:Y for R = H and F while for R = Cl, $\Delta^2E(BeR_2{:}Ar)$ is more important than $\Delta^2E(BeR_2{:}Y)$. The negative value of Δ^3E,

which indicates strong cooperativity, ranges between −21 and −35 kJ/mol in the C_6H_6 complexes and between −13 and −24 kJ/mol in the C_6F_6 ones. The $\Delta^2E(BeR_2:Ar)$ term is always larger in absolute value in the ternary complexes than in the binary ones while the $\Delta^2E(Ar:Y)$ one is slightly smaller in absolute value in the ternary than in the corresponding binary complexes.

Table 7. Many body Interaction energy (MBIE) partition term (kJ/mol) in the ternary systems *.

System	Er(Ar)	Er(BeR_2)	$\Delta^2E(BeR_2:Ar)$	$\Delta^2E(Ar:Y)$	$\Delta^2E(BeR_2:Y)$	$\Delta^3E(BeR_2:Ar:Y)$
$BeH_2:C_6H_6:Br^-$	2.1	25.8	−48.2	−34.5	−4.3	−21.1
$BeH_2:C_6H_6:Cl^-$	2.6	26.5	−48.7	−36.5	−4.5	−22.6
$BeF_2:C_6H_6:Br^-$	2.5	43.3	−81.7	−33.8	−11.0	−24.0
$BeF_2:C_6H_6:Cl^-$	3.0	44.3	−82.3	−35.8	−11.5	−25.6
$BeCl_2:C_6H_6:Br^-$	3.4	58.4	−103.0	−33.1	−11.6	−32.8
$BeCl_2:C_6H_6:Cl^-$	4.0	59.3	−103.6	−35.1	−12.1	−34.8
$BeH_2:C_6F_6:Br^-$	1.7	12.4	−16.1	−65.2	−16.7	−12.9
$BeH_2:C_6F_6:Cl^-$	1.8	13.5	−16.3	−66.3	−18.3	−13.5
$BeF_2:C_6F_6:Br^-$	2.4	29.2	−32.7	−64.2	−32.3	−15.1
$BeF_2:C_6F_6:Cl^-$	2.4	30.4	−33.1	−65.2	−34.7	−15.4
$BeCl_2:C_6F_6:Br^-$	4.3	42.2	−49.5	−63.5	−33.0	−22.9
$BeCl_2:C_6F_6:Cl^-$	4.3	43.8	−50.2	−64.5	−35.5	−23.8

* The sum of these terms is equal to the binding energy.

The topology of the molecular graph of the $BeR_2:C_6H_6:Y^-$ complexes is similar to the sum of those of the corresponding dimers. However the electron density values in the intermolecular BCPs (Table 8) are larger in the ternary complexes than in the corresponding binary ones [0.033 *vs.* 0.0025 au in the Be-π BCP and 0.013 *vs.* 0.010 in the Cl···HC interaction in the $BeCl_2:C_6H_6:Cl^-$ complex and its corresponding binary complexes, Figures 2–4] in agreement with the shorter intermolecular distances found in the former complexes and the relationship between the electron density at the BCP and the interatomic distance [60–66], and with the negative values of the Δ^3E terms. As a consequence of the substantial reinforcement of both the beryllium bonds and the interaction between the aromatic and the anion Y^- on going from the binary complexes to the triads, the molecular graph of the triads $BeR_2:C_6F_6:Y^-$, presents a single intermolecular BCP between the anion and the aromatic ring (Figure 4) in contrast to the six BCPs found in the binary complexes (Figure 3) and a BCP connecting the beryllium atom with the aromatic ring while in the binary complexes the two BCPs were between the R groups and the aromatic ring. Consistently, for the $BeR_2:C_6H_6:Y^-$, both the electron density at the BCP connecting the beryllium atom with the aromatic ring and at the $CH\cdots Y^-$ hydrogen bonds are much larger in the triad than in the corresponding binary complexes.

Table 8. AIM parameters (in au) for the BCPs corresponding to the Be···π and π···Y interactions in the ternary systems, the electron density, ρ_{BCP}, its Laplacian, $\nabla^2\rho_{BCP}$, and the total electron energy density, H_{BCP}.

System	Be···π			π···Y⁻		
	ρ_{BCP}	$\nabla^2\rho_{BCP}$	H_{BCP}	ρ_{BCP}	$\nabla^2\rho_{BCP}$	H_{BCP}
BeH_2:C_6H_6: Br^-	0.0224	0.0278	−0.0059	0.0111	0.0288	0.0005
BeH_2:C_6H_6:Cl^-	0.0227	0.0295	−0.0060	0.0123	0.0347	0.0007
BeF_2:C_6H_6:Br^-	0.0280	0.0860	−0.0048	0.0115	0.0299	0.0005
BeF_2:C_6H_6:Cl^-	0.0283	0.0872	−0.0048	0.0128	0.0362	0.0007
$BeCl_2$:C_6H_6 :Br^-	0.0326	0.0974	−0.0065	0.0120	0.0314	0.0005
$BeCl_2$:C_6H_6:Cl^-	0.0330	0.0990	−0.0070	0.0130	0.0380	0.001
BeH_2:C_6F_6:Br^-	0.0164	0.0182	−0.0041	0.0131	0.0364	0.0011
BeH_2:C_6F_6:Cl^-	0.0169	0.0190	−0.0043	0.0146	0.0455	0.0016
BeF_2:C_6F_6:Br^-	0.0222	0.0373	−0.0060	0.0140	0.0399	0.0012
BeF_2:C_6F_6:Cl^-	0.0226	0.0409	−0.0060	0.0155	0.0494	0.0017
$BeCl_2$:C_6F_6:Br^-	0.0252	0.0336	−0.0082	0.0147	0.0421	0.0012
$BeCl_2$:C_6F_6:Cl^-	0.0257	0.0377	−0.0082	0.0163	0.0524	0.0018

Similar reinforcements of both non-covalent interactions become evident when the NBO analysis is employed, reflected in much larger charge transfer towards the beryllium derivative from both the anion and the aromatic systems (Table 9). At the same time, the second order perturbation analysis shows an increment of the charge transferred from the C-C bonds of the aromatic systems towards the empty ones of the beryllium that corresponds to E(2) stabilization values of 98 and 21 kJ/mol in the BeH_2:C_6X_6:Cl^-, with X = H and F, respectively.

Table 9. Charge (e) of the monomers in the ternary complex.

System	Aromatic	BeR_2	Y^-
BeH_2:C_6H_6: Br^-	0.087	−0.124	−0.963
BeH_2:C_6H_6:Cl^-	0.088	−0.126	−0.962
BeF_2:C_6H_6:Br^-	0.058	−0.010	−0.959
BeF_2:C_6H_6:Cl^-	0.059	−0.101	−0.958
$BeCl_2$:C_6H_6 :Br^-	0.115	−0.161	−0.953
$BeCl_2$:C_6H_6:Cl^-	0.117	−0.163	−0.953
BeH_2:C_6F_6:Br^-	0.067	−0.104	−0.963
BeH_2: C_6F_6:Cl^-	0.070	−0.107	−0.962
BeF_2: C_6F_6:Br^-	0.116	−0.167	−0.949
BeF_2: C_6F_6:Cl^-	0.120	−0.172	−0.948
$BeCl_2$: C_6F_6:Br^-	0.060	−0.102	−0.958
$BeCl_2$: C_6F_6:Cl^-	0.063	−0.107	−0.957

4. Conclusions

Our MP2/aug′-cc-pVDZ theoretical survey of the complexes formed by two aromatic systems (C_6H_6 and C_6F_6) when interacting simultaneously with beryllium derivatives (BeH_2, BeF_2 and $BeCl_2$) and anions (Cl^- and Br^-) shows that the shape of the complexes depends on the aromatic ring. C_6H_6

yields complexes where the anions are practically lying in the molecular plane of the aromatic system, and are stabilized by CH···Y^- hydrogen bonds. Conversely, for C_6F_6 complexes, the Y^- anions are located along the C_6 axis and above the ring to favor the interaction with the π electrons. The beryllium derivatives are close to one of the C-C bonds of the aromatic moiety in all the complexes (binary and ternary) with C_6H_6 while in the C_6F_6 binary complexes they are much farther away, due to the much smaller electron donor capacity of C_6F_6. Strong cooperative effects are found when comparing the interactions in the triads with those in the corresponding binary complexes. Indeed, the electronic density distribution of the BeR_2:aromatic:Y^- ternary complexes reflects these cooperative effects by a significant increase of the electron density at the intermolecular BCPs between the beryllium derivative and the aromatic system and between the aromatic system and the Y^- anion. Also the MBIE analysis accounts for this cooperativity mirrored in significant negative values of the three-body interaction energy, Δ^3E. Although these interactions have a clear electrostatic component, they also show significant polarization effects which lead to significant deformations of the BeR_2 moiety, which becomes clearly bent with longer Be-R bonds, through a charge transfer to the empty p orbitals of Be and to the σ_{BeR}* antibonding orbitals. This cooperativity is in agreement with the combination of π-anion contacts with other weak interactions (halogen and hydrogen bonds) already described in the literature [67].

Supplementary Materials

Supplementary materials can be accessed at: http://www.mdpi.com/1420-3049/20/06/9961/s1.

Acknowledgments

This work has been partially supported by the Ministerio de Economía y Competitividad (Projects No. CTQ2012-35513-C02 and CTQ2013-43698-P), the Project FOTOCARBON, Ref.: S2013/MIT-2841 of the Comunidad Autónoma de Madrid, and by the CMST COST Action CM1204. A generous allocation of computing time at the CTI (CSIC) and at the CCC of the UAM is also acknowledged.

Author Contributions

Ibon Alkorta and Manuel Yáñez conceived and designed the calculations; Marta Marín-Luna performed the calculations; Marta Marín-Luna, Ibon Alkorta, José Elguero, Otilia Mó and Manuel Yáñez analyzed the data and wrote the paper.

Conflicts of Interest

The authors declare no conflict of interest.

References

1. Quiñonero, D.; Garau, C.; Rotger, C.; Frontera, A.; Ballester, P.; Costa, A.; Deyà, P.M. Anion–π Interactions: Do They Exist? *Angew. Chem. Int. Ed.* **2002**, *41*, 3389–3392.
2. Mascal, M.; Armstrong, A.; Bartberger, M.D. Anion-Aromatic Bonding: A Case for Anion Recognition by π-Acidic Rings. *J. Am. Chem. Soc.* **2002**, *124*, 6274–6276.

3. Alkorta, I.; Rozas, I.; Elguero, J. Interaction of Anions with Perfluoro Aromatic Compounds. *J. Am. Chem. Soc.* **2002**, *124*, 8593–8598.
4. Allen, F. The Cambridge Structural Database: A quarter of a million crystal structures and rising. *Acta Crystallogr. B* **2002**, *58*, 380–388.
5. Berryman, O.B.; Johnson, D.W. Experimental evidence for interactions between anions and electron-deficient aromatic rings. *Chem. Commun.* **2009**, 3143–3153.
6. Giese, M.; Albrecht, M.; Valkonen, A.; Rissanen, K. The pentafluorophenyl group as p-acceptor for anions: A case study. *Chem. Sci.* **2015**, *6*, 354–359.
7. Berryman, O.B.; Bryantsev, V.S.; Stay, D.P.; Johnson, D.W.; Hay, B.P. Structural Criteria for the Design of Anion Receptors: The Interaction of Halides with Electron-Deficient Arenes. *J. Am. Chem. Soc.* **2007**, *129*, 48–58.
8. Ballester, P. Anions and π-aromatic systems. Do they interact attractively? In *Recognition of Anions*; Vilar, R., Ed.; Springer Berlin Heidelberg: Berlin, Germany, 2008; Volume 129, pp. 127–174.
9. Quiñonero, D.; Frontera, A.; Deyà, P.M. Anion-π interactions in molecular recognition. In *Anion Coordination Chemistry*; Wiley-VCH Verlag GmbH & Co. KGaA: Weinheim, Gemany, 2011; pp. 321–361.
10. Wang, D.X.; Wang, M.X. Anion-π Interactions: Generality, Binding Strength, and Structure. *J. Am. Chem. Soc.* **2013**, *135*, 892–897.
11. Berryman, O.B.; Hof, F.; Hynes, M.J.; Johnson, D.W. Anion-p interaction augments halide binding in solution. *Chem. Commun.* **2006**, 506–508.
12. Albrecht, M.; Wessel, C.; de Groot, M.; Rissanen, K.; Lüchow, A. Structural Versatility of Anion-π Interactions in Halide Salts with Pentafluorophenyl Substituted Cations. *J. Am. Chem. Soc.* **2008**, *130*, 4600–4601.
13. Garau, C.; Quinonero, D.; Frontera, A.; Ballester, P.; Costa, A.; Deya, P.M. Anion-p interactions: Must the aromatic ring be electron deficient? *New J. Chem.* **2003**, *27*, 211–214.
14. Alkorta, I.; Elguero, J. Aromatic Systems as Charge Insulators: Their Simultaneous Interaction with Anions and Cations. *J. Phys. Chem. A* **2003**, *107*, 9428–9433.
15. Quiñonero, D.; Frontera, A.; Garau, C.; Ballester, P.; Costa, A.; Deyà, P.M. Interplay Between Cation-π, Anion-π and π-π Interactions. *ChemPhysChem* **2006**, *7*, 2487–2491.
16. Alkorta, I.; Quiñonero, D.; Garau, C.; Frontera, A.; Elguero, J.; Deyà, P.M. Dual Cation and Anion Acceptor Molecules. The Case of the (η6-C6H6)(η6C6F6)Cr(0) Complex. *J. Phys. Chem. A* **2007**, *111*, 3137–3142.
17. Frontera, A.; Quinonero, D.; Costa, A.; Ballester, P.; Deya, P.M. MP2 study of cooperative effects between cation-p, anion-p and p-p interactions. *New J. Chem.* **2007**, *31*, 556–560.
18. Quiñonero, D.; Frontera, A.; Deyà, P.M.; Alkorta, I.; Elguero, J. Interaction of positively and negatively charged aromatic hydrocarbons with benzene and triphenylene: Towards a model of pure organic insulators. *Chem. Phys. Lett.* **2008**, *460*, 406–410.
19. Frontera, A.; Quiñonero, D.; Deyà, P.M. Cation–π and anion–π interactions. *WIREs Comput. Mol. Sci.* **2011**, *1*, 440–459.
20. Mandal, T.K.; Samanta, S.; Chakraborty, S.; Datta, A. An Interplay of Cooperativity between Cation···π, Anion···π and CH···Anion Interactions. *ChemPhysChem* **2013**, *14*, 1149–1154.

21. Lucas, X.; Quiñonero, D.; Frontera, A.; Deyà, P.M. Counterintuitive Substituent Effect of the Ethynyl Group in Ion-π Interactions. *J. Phys. Chem. A* **2009**, *113*, 10367–10375.
22. Naumkin, F.Y. Trapped-molecule charge-transfer complexes with huge dipoles: M-C2F6-X (M = Na to Cs, X = Cl to I). *Phys. Chem. Chem. Phys.* **2008**, *10*, 6986–6990.
23. Trujillo, C.; Sánchez-Sanz, G.; Alkorta, I.; Elguero, J. Simultaneous Interactions of Anions and Cations with Cyclohexane and Adamantane: Aliphatic Cyclic Hydrocarbons as Charge Insulators. *J. Phys. Chem. A* **2011**, *115*, 13124–13132.
24. Estarellas, C.; Frontera, A.; Quiñonero, D.; Alkorta, I.; Deyà, P.M.; Elguero, J. Energetic *vs* Synergetic Stability: A Theoretical Study. *J. Phys. Chem. A* **2009**, *113*, 3266–3273.
25. Alkorta, I.; Blanco, F.; Elguero, J.; Estarellas, C.; Frontera, A.; Quiñonero, D.; Deyà, P.M. Simultaneous Interaction of Tetrafluoroethene with Anions and Hydrogen-Bond Donors: A Cooperativity Study. *J. Chem. Theor. Comput.* **2009**, *5*, 1186–1194.
26. Yáñez, M.; Sanz, P.; Mó, O.; Alkorta, I.; Elguero, J. Beryllium Bonds, Do They Exist? *J. Chem. Theor. Comput.* **2009**, *5*, 2763–2771.
27. Mó, O.; Yáñez, M.; Alkorta, I.; Elguero, J. Modulating the Strength of Hydrogen Bonds through Beryllium Bonds. *J. Chem. Theor. Comput.* **2012**, *8*, 2293–2300.
28. Yáñez, M.; Mó, O.; Alkorta, I.; Elguero, J. Can Conventional Bases and Unsaturated Hydrocarbons Be Converted into Gas-Phase Superacids That Are Stronger than Most of the Known Oxyacids? The Role of Beryllium Bonds. *Chem. Eur. J.* **2013**, *19*, 11637–11643.
29. Yáñez, M.; Mó, O.; Alkorta, I.; Elguero, J. Spontaneous ion-pair formation in the gas phase induced by Beryllium bonds. *Chem. Phys. Lett.* **2013**, *590*, 22–26.
30. Mó, O.; Yáñez, M.; Alkorta, I.; Elguero, J. Enhancing and modulating the intrinsic acidity of imidazole and pyrazole through beryllium bonds. *J. Mol. Model.* **2013**, *19*, 4139–4145.
31. Montero-Campillo, M.M.; Lamsabhi, A.; Mó, O.; Yáñez, M. Modulating weak intramolecular interactions through the formation of beryllium bonds: Complexes between squaric acid and BeH2. *J. Mol. Model.* **2013**, *19*, 2759–2766.
32. Albrecht, L.; Boyd, R.J.; Mó, O.; Yáñez, M. Changing Weak Halogen Bonds into Strong Ones through Cooperativity with Beryllium Bonds. *J. Phys. Chem. A* **2014**, *118*, 4205–4213.
33. Martin-Somer, A.; Mo, O.; Yanez, M.; Guillemin, J.C. Acidity enhancement of unsaturated bases of group 15 by association with borane and beryllium dihydride. Unexpected boron and beryllium Bronsted acids. *Dalton Transact.* **2015**, *44*, 1193–1202.
34. Alkorta, I.; Elguero, J.; Mo, O.; Yanez, M.; Del Bene, J.E. Using beryllium bonds to change halogen bonds from traditional to chlorine-shared to ion-pair bonds. *Phys. Chem. Chem. Phys.* **2015**, *17*, 2259–2267.
35. Villanueva, E.F.; Mo, O.; Yanez, M. On the existence and characteristics of [small pi]-beryllium bonds. *Phys. Chem. Chem. Phys.* **2014**, *16*, 17531–17536.
36. Møller, C.; Plesset, M.S. Note on an Approximation Treatment for Many-Electron Systems. *Phys. Rev.* **1934**, *46*, 618–622.
37. Dunning, T.H. Gaussian-Basis Sets for Use in Correlated Molecular Calculations .1. The Atoms Boron through Neon and Hydrogen. *J. Chem. Phys.* **1989**, *90*, 1007–1023.

38. Frisch, M.J.; Trucks, G.W.; Schlegel, H.B.; Scuseria, G.E.; Robb, M.A.; Cheeseman, J.R.; Scalmani, G.; Barone, V.; Mennucci, B.; Petersson, G.A.; *et al. Gaussian 09*; Gaussian, Inc.: Wallingford, CT, USA, 2009.
39. Hankins, D.; Moskowitz, J.W.; Stillinger, F.H. Water Molecule Interactions. *J. Chem. Phys.* **1970**, *53*, 4544–4554.
40. Xantheas, S.S. Ab initio studies of cyclic water clusters (H2O)n, *n* = 1–6. II. Analysis of many-body interactions. *J. Chem. Phys.* **1994**, *100*, 7523–7534.
41. Bader, R.F.W. *Atoms in Molecules: A Quantum Theory*. Clarendon Press: Oxford, UK, 1990.
42. Popelier, P.L.A. *Atoms in Molecules. An Introduction*. Prentice Hall: Harlow, UK, 2000.
43. Keith, T.A. *AIMAll*, Version 11.10.16; TK Gristmill Software: Overland Park KS, USA, 2011.
44. Reed, A.E.; Curtiss, L.A.; Weinhold, F. Intermolecular Interactions from a Natural Bond Orbital, Donor-Acceptor Viewpoint. *Chem. Rev.* **1988**, *88*, 899–926.
45. Glendening, E.D.; Reed, A.E.; Carpenter, J.E.; Weinhold, F. *NBO*, Version 3.1.; Gaussian Inc. Wallingford, CT, USA, 1988.
46. Kruszewski, J.; Krygowski, T.M. Definition of aromaticity basing on the harmonic oscillator model. *Tetrahedron Lett.* **1972**, *13*, 3839–3842.
47. Krygowski, T.M.; Cyrański, M. Separation of the energetic and geometric contributions to the aromaticity of π-electron carbocyclics. *Tetrahedron* **1996**, *52*, 1713–1722.
48. Alkorta, I.; Rozas, I.; Elguero, J. An Attractive Interaction between the π-Cloud of C6F6 and Electron-Donor Atoms. *J. Org. Chem.* **1997**, *62*, 4687–4691.
49. Mahadevi, A.S.; Sastry, G.N. Cation–π Interaction: Its Role and Relevance in Chemistry, Biology, and Material Science. *Chem. Rev.* **2013**, *113*, 2100–2138.
50. Tarakeshwar, P.; Lee, S.J.; Lee, J.Y.; Kim, K.S. Benzene-hydrogen halide interactions: Theoretical studies of binding energies, vibrational frequencies, and equilibrium structures. *J. Chem. Phys.* **1998**, *108*, 7217–7223.
51. Ma, J.C.; Dougherty, D.A. The Cation-π Interaction. *Chem. Rev.* **1997**, *97*, 1303–1324.
52. Cabarcos, O.M.; Weinheimer, C.J.; Lisy, J.M. Competitive solvation of K^+ by benzene and water: Cation-π interactions and π-hydrogen bonds. *J. Chem. Phys.* **1998,** *108*, 5151–5154.
53. Saggu, M.; Levinson, N.M.; Boxer, S.G. Experimental Quantification of Electrostatics in X–H···π Hydrogen Bonds. *J. Am. Chem. Soc.* **2012**, *134*, 18986–18997.
54. Alkorta, I.; Rozas, I.; Jimeno, M.; Elguero, J.A Theoretical and Experimental Study of the Interaction of C6F6 with Electron Donors. *Struct. Chem.* **2001**, *12*, 459–464.
55. Battaglia, M.R.; Buckingham, A.D.; Williams, J.H. The electric quadrupole moments of benzene and hexafluorobenzene. *Chem. Phys. Lett.* **1981**, *78*, 421–423.
56. Rozas, I.; Alkorta, I.; Elguero, J. Behavior of Ylides Containing N, O, and C Atoms as Hydrogen Bond Acceptors. *J. Am. Chem. Soc.* **2000**, *122*, 11154–11161.
57. Emmeluth, C.; Poad, B.L.J.; Thompson, C.D.; Bieske, E.J. Interactions between the Chloride Anion and Aromatic Molecules: Infrared Spectra of the Cl^-–$C_6H_5CH_3$, Cl^-–$C_6H_5NH_2$ and Cl^-–C_6H_5OH Complexes. *J. Phys. Chem. A* **2007**, *111*, 7322–7328.
58. Loh, Z.M.; Wilson, R.L.; Wild, D.A.; Bieske, E.J.; Zehnacker, A. Cl^-–C_6H_6, Br^-–C_6H_6, and I^-–C_6H_6 anion complexes: Infrared spectra and ab initio calculations. *J. Chem. Phys.* **2003**, *119*, 9559–9567.

59. Thompson, C.D.; Poad, B.L.J.; Emmeluth, C.; Bieske, E. Infrared spectra of Cl^{-}–$(C_6H_6)_m$ m = 1, 2. *Chem. Phys. Lett.* **2006,** *428*, 18–22.
60. Espinosa, E.; Alkorta, I.; Elguero, J.; Molins, E. From weak to strong interactions: A comprehensive analysis of the topological and energetic properties of the electron density distribution involving X–H···F–Y systems. *J. Chem. Phys.* **2002**, *117*, 5529–5542.
61. Knop, O.; Boyd, R.J.; Choi, S.C. Sulfur-sulfur bond lengths, or can a bond length be estimated from a single parameter? *J. Am. Chem. Soc.* **1988**, *110*, 7299–7301.
62. Alkorta, I.; Barrios, L.; Rozas, I.; Elguero, J. Comparison of models to correlate electron density at the bond critical point and bond distance. *J. Mol. Struct. THEOCHEM* **2000**, *496*, 131–137.
63. Knop, O.; Rankin, K.N.; Boyd, R.J. Coming to Grips with N–H···N Bonds. 1. Distance Relationships and Electron Density at the Bond Critical Point. *J. Phys. Chem. A* **2001**, *105*, 6552–6566.
64. Knop, O.; Rankin, K.N.; Boyd, R.J. Coming to Grips with N–H···N Bonds. 2. Homocorrelations between Parameters Deriving from the Electron Density at the Bond Critical Point1. *J. Phys. Chem. A* **2003**, *107*, 272–284.
65. Mata, I.; Alkorta, I.; Molins, E.; Espinosa, E. Universal Features of the Electron Density Distribution in Hydrogen-Bonding Regions: A Comprehensive Study Involving H···X (X=H, C, N, O, F, S, Cl, π) Interactions. *Chem. Eur. J.* **2010**, *16*, 2442–2452.
66. Alkorta, I.; Solimannejad, M.; Provasi, P.; Elguero, J. Theoretical Study of Complexes and Fluoride Cation Transfer between $N2F^{+}$ and Electron Donors. *J. Phys. Chem. A* **2007**, *111*, 7154–7161.
67. Alkorta, I.; Blanco, F.; Deyà, P.; Elguero, J.; Estarellas, C.; Frontera, A.; Quiñonero, D. Cooperativity in multiple unusual weak bonds. *Theor. Chem. Acc.* **2010**, *126*, 1–14.

Sample Availability: Not available.